tvst

Article

Quantitative Optical Coherence Tomography Angiography Parameters in Type 1 Macular Neovascularization Secondary to Age-Related Macular Degeneration

Alessandro Arrigo[1], Emanuela Aragona[1], Carlo Di Nunzio[1], Francesco Bandello[1], and Maurizio Battaglia Parodi[1]

[1] Department of Ophthalmology, IRCCS San Raffaele Hospital, Vita-Salute University, Milan, Italy

Correspondence: Alessandro Arrigo, Department of Ophthalmology, IRCCS San Raffaele Hospital, University Vita-Salute, via Olgettina 60, Milan, 20132, Italy. e-mail: alessandro.arrigo@hotmail.com

Received: April 4, 2020
Accepted: August 5, 2020
Published: August 31, 2020

Keywords: age-related macular degeneration; optical coherence tomography (OCT); optical coherence tomography angiography (OCTA); macular neovascularization (MNV); vessel density; vessel tortuosity; vessel dispersion

Citation: Arrigo A, Aragona E, Di Nunzio C, Bandello F, Parodi MB. Quantitative optical coherence tomography angiography parameters in type 1 macular neovascularization secondary to age-related macular degeneration. Trans Vis Sci Tech. 2020;9(9):48, https://doi.org/10.1167/tvst.9.9.48

Purpose: The purpose of this paper was to study type 1 macular neovascularization (MNV) quantitative optical coherence tomography (OCT) angiography (OCTA) features by means of advanced postprocessing analyses.

Methods: We recruited patients affected by naïve type 1 MNV secondary to age-related macular degeneration (AMD) and age-matched controls. All patients underwent ophthalmologic examination and multimodal imaging. They were treated with pro-re-nata anti-VEGF injections. The ensuing follow-up lasted 24 months. Quantitative OCT and OCTA parameters were statistically analyzed to obtain cutoff values able to distinguish two clinically different patient subgroups. Main outcome measures were best-corrected visual acuity (BCVA), central macular thickness, vessel density of superficial, deep and choriocapillaris plexa, vessel tortuosity (VT) of MNV, vessel dispersion of MNV, number of injections, blooding, pigment epithelium detachment, subretinal fluid, photoreceptor elongation, subretinal fibrosis, and outer retinal atrophy.

Results: Ninety-one eyes (91 patients; 49 men; mean age 78 $\pm$ 7 years) and 91 control eyes were included. Mean logarithm of the minimum angle of resolution (logMAR) BCVA was 0.46 $\pm$ 0.56 at baseline, increasing up to 0.29 $\pm$ 0.30 after 2 years of treatment ($P <$ 0.01). The mean number of intravitreal injections was 7.1 $\pm$ 2.0 during the first year and 4.5 $\pm$ 1.4 during the second year. A baseline VT cutoff of 8.40 detected two patients' subgroups differing significantly in terms of BCVA improvement after 2 years of treatment.

Conclusions: OCTA-based classification of type 1 MNV, performed at baseline, provided useful information in terms of the functional outcome achievable after 24 months of anti-VEGF treatment.

Translational Relevance: Quantitative OCTA-based classification of type 1 MNV, performed at baseline, provided useful information in terms of the functional outcome achievable after 24 months of anti-VEGF treatment.

Introduction

Type 1 macular neovascularization (MNV) is the most frequent MNV occurring as a complication of age-related macular degeneration (AMD).[1] The term "type 1" is used in reference to the growth of the neovascularization below the retinal pigment epithelium (RPE), which causes a masking effect on fluorescein angiography (FA) in the early stages and the onset of leakage phenomena and typical "pin-points" - hyperfluorescent spots - during the late stages.[2] Indocyanine green angiography (ICGA) usually serves to reveal the plaque pattern characterizing type 1 MNV.[2,3] The relatively recent introduction of a noninvasive technique known as optical coherence tomography (OCT) angiography (OCTA) has supplied further details, as this technique is able to reconstruct the intricate neovascular network growing within the sub-RPE space.[3]

Anti-VEGF intravitreal injections are widely known to be an effective treatment for type 1 MNV.[2] However, in clinical practice, patients display diverse responses to treatment, thus leading to variable visual outcomes. Although several studies have tried to correlate imaging findings with clinically useful information,[4–6] the functional characterization of type 1 MNV remains a challenging undertaking. A recent article showed that quantitative OCTA parameters can separate different MNV subgroups, helping to predict the 1-year functional outcome after anti-VEGF treatment.[7]

The purpose of the present study is to describe the quantitative OCTA characterization of the vascular patterns of type 1 MNV treated with anti-VEGF injections over a 24-month follow-up.

Methods

The study was designed as an interventional, prospective case series with a 24-month follow-up. All the patients were recruited at the Ophthalmology Unit of San Raffaele Hospital, Milan, between January 2016 and January 2017. Signed informed consent was obtained from all patients. The whole study was conducted in accordance with the Declaration of Helsinki and approved by the Ethical Committee of the Vita-Salute San Raffaele University in Milan. All consecutive patients with AMD with naïve subfoveal type 1 MNV were recruited and underwent ranibizumab 0.5 mg intravitreal treatment, including a loading phase of 3 injections followed by further anti-VEGF injections, in accordance with a pro-re-nata regimen.

The inclusion criteria were: naïve type 1 MNV secondary to AMD, as identified on FA and confirmed by means of ICGA (Spectralis HRA+OCT; Heidelberg Engineering, Heidelberg, Germany).

The following exclusion criteria were considered: retinal angiomatous proliferations, polypoidal choroidal vasculopathy, pigment epithelium detachment (PED) > 250 µm, detected on structural OCT because OCTA resolution is not high enough to identify the lesions.[8] We also excluded patients with high media opacity, any other type of retinal or optic nerve diseases, ophthalmologic surgery within the last 3 months, and any systemic condition potentially affecting the analyses.

Ophthalmologic examination included best-corrected visual acuity (BCVA) measurement using standard early treatment diabetic retinopathy study (ETDRS) charts, slit lamp biomicroscopy of anterior and posterior segments, and Goldmann applanation tonometry. Fundus and structural OCT images were acquired by means of Spectralis HRA+OCT, Heidelberg, Germany. Structural OCT acquisition protocol included raster, radial and dense scans with a high number of frames (ART > 25), and enhanced depth imaging (EDI). Structural OCT scans were used to measure central macular thickness (CMT) at baseline and after the 2-year follow-up.

Baseline OCTA images were obtained by means of a swept-source DRI OCT Triton (Topcon Corporation, Tokyo, Japan), with both high-resolution 3 × 3-mm and 4.5 × 4.5-mm acquisitions being included.

Automatic segmentation into superficial capillary plexa (SCP), deep capillary plexa (DCP), and choriocapillaris (CC) was obtained from OCTA acquisitions. Each segmentation was carefully inspected and, if necessary, manually corrected by two expert ophthalmologists (M.B.P. and A.A.), taking only high-quality images (Topcon quality index > 80) into consideration.

All reconstructions were loaded in ImageJ software (https://imagej.net/Welcome) to calculate vessel density (VD). The "Adjust threshold" tool was used in ImageJ to highlight the blood vessels and to reduce the noise. The pipeline adopted for image binarization was: image loading -> adjust threshold -> automatic mean threshold. VD was calculated to determine the ratio of white pixels to black. The foveal avascular zone was manually segmented and excluded. Vessel tortuosity (VT) and vessel dispersion (VDisp) were measured for each segmented MNV network.[7] VT is defined as the ratio of the shortest pathway to the straight line length, providing information about the vascular perfusion.[9,10] It was calculated on the basis of an ImageJ automatic pipeline and included different consecutive passages that were independent from the researcher performing the analysis. The key passages included binarization (as previously described for vessel density), skeletonization (an automated method that considers each vessel as a line, performed by means of a "Skeletonize3D" pipeline included in ImageJ), and branch recognition, followed by the calculation of the Euclidean distance for each line, which is the final measure of the tortuosity. The Euclidean distance is the ratio between each line's length and the shortest linear distance between the initial and the final point. We used Strahler Analysis to accurately pick out each root, thus reducing possible bias (https://imagej.net/Strahler_Analysis#Root_Detection).[11] In this way, it was possible to determine the geometrical properties of each MNV.[12] The pipeline adopted to extract MNV VT was: analyze -> skeleton -> analyze skeleton (Fig. 1).

VDisp is defined as a measure of the space-filling of a given vascular tree and provides information about the vascular network disorganization.[12,13] VDisp

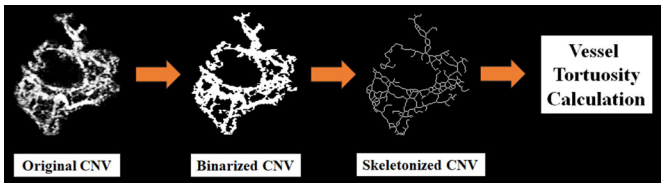

Figure 1. Pipeline for vessel tortuosity calculation. The process includes: MNV binarization through a mean threshold, MNV skeletonization by using "Skeletonize3D" function provided by ImageJ, followed by analysis of the skeletonized image through the "AnalyzeSkeleton" ImageJ pipeline. More details are provided in the text.

was calculated assuming that all vessels follow certain directions that can be studied through a Gaussian function. The measure of data dispersion, defined as the standard deviation from the Gaussian distribution, may express the disorganization of the MNV vascular network.[14] The calculation was done on skeletonized reconstructions by applying the "Directionality" ImageJ function and extracting data dispersion values.[15,16] The pipeline adopted to extract MNV VDisp was: analyze -> directionality -> Fourier components method -> dispersion calculation.

We performed a receiver operating characteristic (ROC) analysis on MNV VT and VDisp values obtained from the neovascular networks, following the same procedure previously reported,[7] in order to place patients into statistically differing subgroups for the final BCVA outcome. In particular, the ROC analysis was conducted considering eyes with a significant gain in visual acuity at the end of the follow-up versus eyes showing stable or worse conditions.

The presence of retinal/subretinal hemorrhages at baseline, as found on biomicroscopic fundus examination, was recorded, and structural OCT was used to detect the presence of subretinal fluid, pigment epithelium detachment, and photoreceptor elongation. Moreover, fundus images and structural OCT were evaluated to assess the development of subretinal fibrosis and outer retinal atrophy. All the parameters were noted as binary results. The presence of intraretinal hyper-reflective foci (HF) were also investigated at the baseline and at the end of the 2-year follow-up. In order to make it easier to quantify HF in clinical settings, we classified HF as follows: 0 (no HF), 1 (< 15 HF), 2 (< 30 HF), 3 (< 45 HF), and 4 (> 45 HF). We assessed the relationship among intraretinal HF, BCVA, and VT values of the MNV. We further categorized patients in accordance with HF changes detected at the end of the follow-up (reduced, stable, or increased HF). We also performed an ROC analysis on HF to detect possible cutoff values that would enable eyes with significant visual acuity gain at the end of the follow-up to be segregated from eyes displaying stable or worse conditions.

The statistical analyses were performed using the 1-way ANOVA test (SPSS, Chicago, IL, USA), with statistical significance set at $P < 0.05$. Post hoc analyses were focused on the analyses of differences between the two subgroups of MNV group 1, MNV group 2, and healthy controls. Owing to the multiple testing, the Bonferroni approach was adopted to account for multiple comparison issues; this choice resulted in an alpha value of $0.05/10 = 0.005$, which was required to obtain an overall alpha value of 0.05.

All OCTA images were captured by two ophthalmologists (M.B.P. and A.A.) at least twice, in order to assess both reproducibility and repeatability for all the considered quantitative parameters.

Reproducibility and repeatability were assessed in accordance with the British Standards Institute and the International Organization for Standardization.[17] Furthermore, we calculated interclass correlation coefficient (ICC) to assess the inter-graders agreement through a two-way random-effects model, provided in SPSS software.

Results

One hundred twelve patients with newly diagnosed type 1 MNV were recruited. Seventy-nine patients were referred by external ophthalmologists, whereas 33 patients were examined in the outpatient departments of our institution. All the patients complained of metamorphopsia and visual acuity deterioration over the previous 30 days. Forty-five patients were already under treatment for MNV in the fellow eye. Twenty-nine patients were excluded owing to high media opacities (14), glaucoma (7), diabetes mellitus (5), and uncontrolled arterial hypertension (3).

As a result, 91 eyes of 91 patients (49 men; mean age 78 ± 7 years) were ultimately involved in the analyses. Mean BCVA was 0.46 ± 0.56 logarithm of the minimum angle of resolution (logMAR) at baseline, which was found to have improved to 0.29 ± 0.30 after 2 years of treatment, with a mean number of 7.1 ± 2.0 and 4.5 ± 1.4 intravitreal injections during the first and second years of follow-up, respectively (total number of injections: 11.6 ± 2.2). These patients were matched by a control group composed of 91 eyes of 91 healthy subjects (46 men; mean age 77 ± 8 years; mean logMAR BCVA 0.0 ± 0.0).

All patients showed type 1 MNV of FA (Fig. 2), with pigment epithelium detachment in 69 eyes (76%). Structural OCT showed the presence of a hyper-

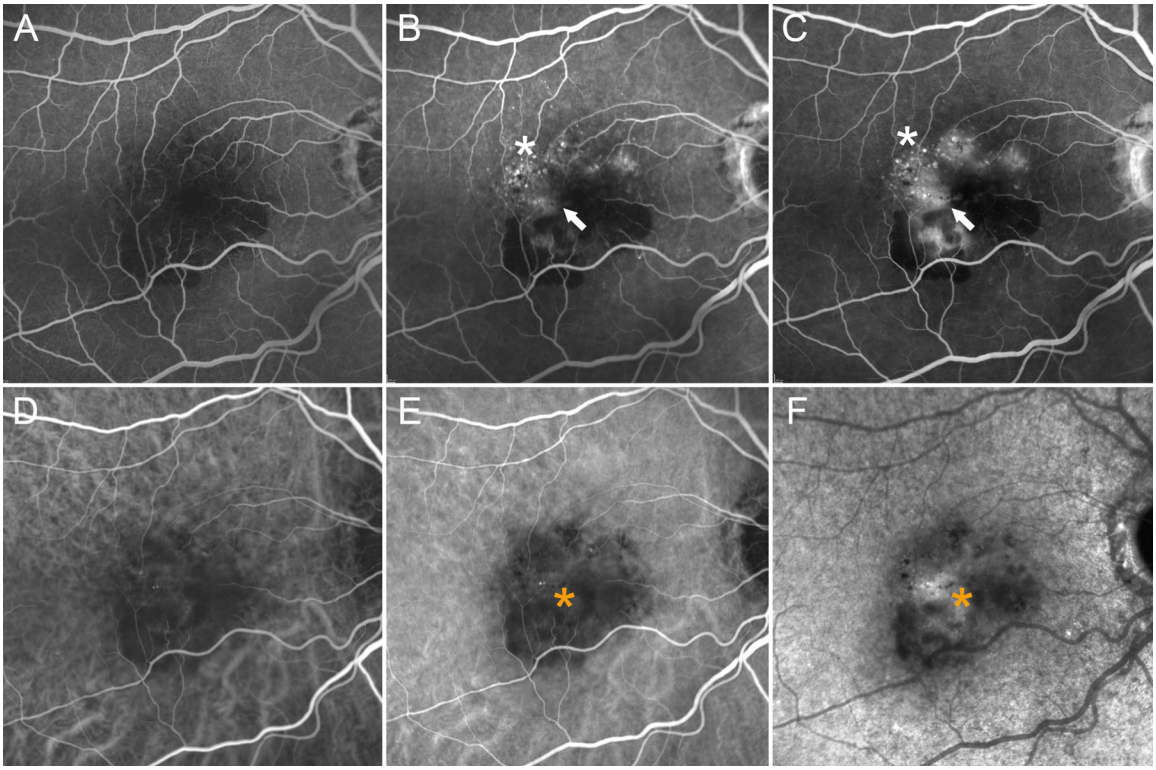

Figure 2. FA and ICGA images in type 1 MNV. FA shows unremarkable changes in the early stage (**A**), whereas increased filling and leakage phenomena (*arrow*), including the typical pinpoint aspect (*white asterisk*), can be observed in the intermediate (**B**) and late stages (**C**). ICGA shows increased perfusion defects from early (**D**) to intermediate (**E**) and late (**F**) stages, with plaque aspect of the neovascular network (*orange asterisk*).

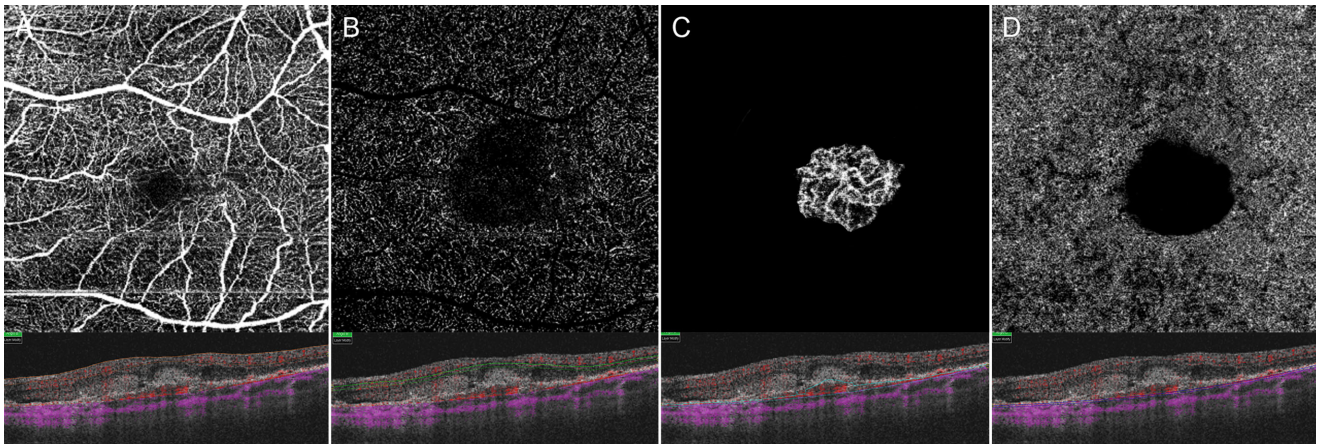

Figure 3. OCTA images in type 1 MNV. The superficial capillary plexus appears preserved (**A**), whereas the deep capillary plexus results rarefied (**B**). A clear neovascular network is reconstructed in (**C**). Choriocapillaris shows normal morphology in the extra-lesional region, whereas the neovascular lesion causes a masking of the perfusion in the involved region (**D**). The correspondent segmentation layers on the OCT B-scans are shown in the lower part of the images.

reflective lesion localized below the RPE, in association with subretinal fluid in all the eyes. OCTA detected the presence of a neovascular network in the sub-RPE space in all cases (Fig. 3). All demographic and clinical data are reported in Table 1.

ROC analysis highlighted the following VT cutoff values: 8.35 (0.846 sensitivity and 0.865 specificity), 8.40 (0.9 sensitivity and 0.898 specificity), and 8.45 (0.868 sensitivity and 0.854 specificity). In accordance with our previous experience, we adopted the VT cutoff

Table 1. Demographic and Clinical Features

	Demographic and Clinical Features				
	Type 1 MNV		Controls		
	Mean	STD	Mean	STD	*P* Value
Age	78	7	76	9	>0.05
Sex (M/F)	49/42		46/45		>0.05
BCVA logMAR baseline	0.46	0.56	0.0	0.0	<0.01
BCVA logMAR 2 y	0.29	0.30			<0.01
No. of injections 2 y	10.91	1.88	0	0	<0.01
CMT baseline	373.76	85.61	296.33	12.80	<0.01
CMT 2 y	346.95	85.19			<0.01
VD SCP baseline	0.38	0,02	0.42	0.02	<0.01
VD DCP baseline	0.36	0.03	0.44	0.01	<0.01
VD CC baseline	0.45	0.04	0.50	0.01	<0.01

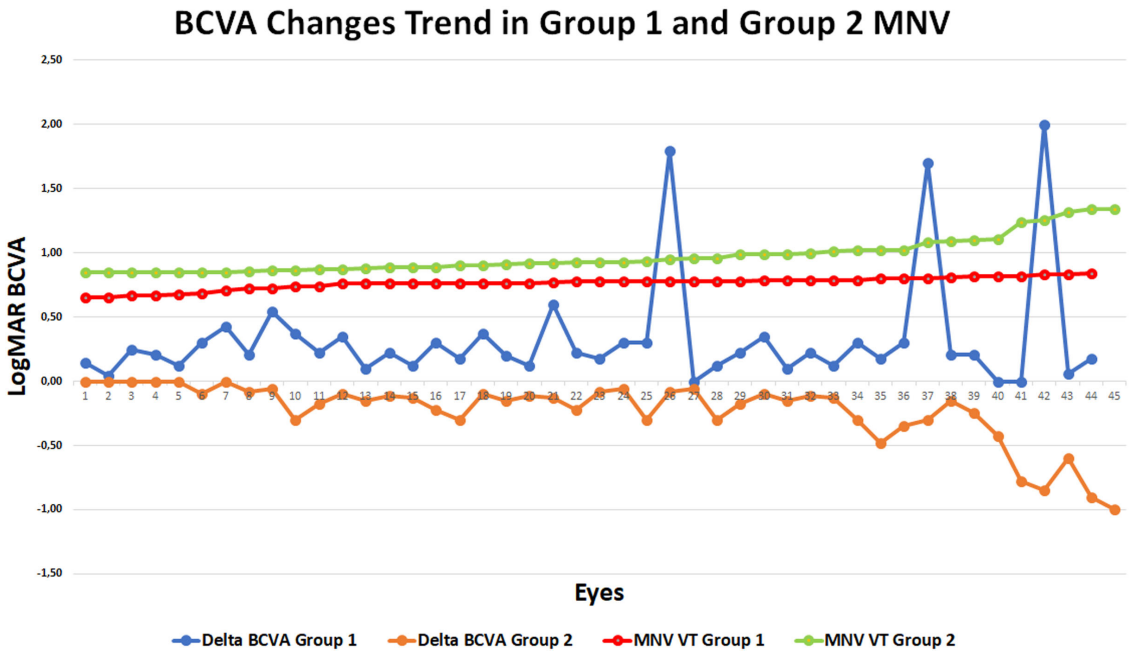

Figure 4. Line plot of VT values, showing that group 1 (*red line*) and group 2 (*green line*) indeed represent two distinct populations of patients affected by type 1 MNV. Moreover, delta BCVA was plotted to highlight how group 1 (*blue line*) shows an improvement, whereas group 2 (*orange line*) reveals a deterioration at the end of the follow-up.

of 8.40 to characterize MNV lesions better. In this way, we were able to isolate a subgroup of low VT (VT < 8.40) and a subgroup showing high VT (VT > 8.40). VT values within the two distinct populations are plotted in Figure 4. Representative cases of the two subgroups are shown in Figure 5 and Figure 6. These two subgroups differed significantly in terms of baseline photoreceptor elongation, subretinal fluid at the 2-year follow-up examination, subretinal fibrosis, and atrophy rate (Table 2). No difference was found between low and high VT subgroups with regard to the number of injections over the first and second years of the follow-up ($P > 0.05$).

Intraretinal HFs were detected in all our patients at baseline, with no statistically significant differences between MNV group 1 and MNV group 2 ($P > 0.05$). In contrast, intraretinal HF proved to be remarkably higher in patients in MNV group 2 (VT > 8.40)

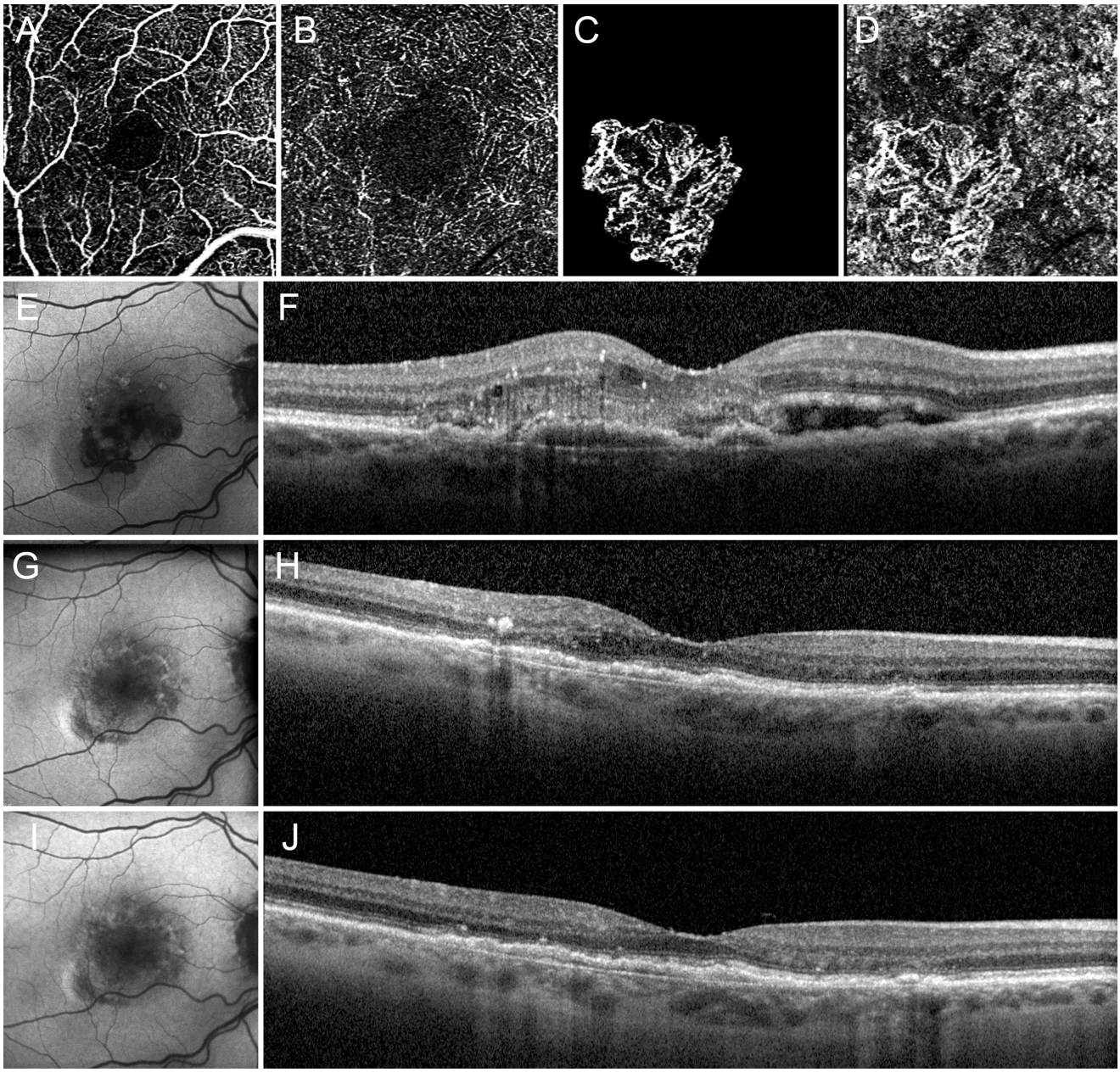

Figure 5. Type 1 MNV case classified as group 1 (VT < 8.40). OCTA clearly reconstructs SCP (**A**), DCP (**B**), MNV (**C**), and CC (**D**). Baseline features are shown in (**E**) and (**F**). After anti-VEGF treatment, exudation was found to be markedly reduced, as was the progression of the outer retinal atrophy at both the 1-year (**G, H**) and 2-year (**I, J**) follow-ups.

($P < 0.01$). Moreover, in group 1 (VT < 8.40) 56% of patients showed reduced HF at the end of the 2-year follow-up, 35% showed stable HF and 9% showed increased HF with respect to baseline. Conversely, intraretinal HFs were found to be considerably higher at the end of the 2-year follow-up in group 2 compared with group 1 ($P < 0.01$).

LogMAR BCVA significantly correlated with the number of HF, both at baseline (Tau coefficient 0.189; $P = 0.02$) and at the 2-year follow-up (Tau coefficient 0.343; $P < 0.001$). Interestingly, MNV VT values correlated with HF number only at 2-year follow-up (Tau coefficient 0.553; $P < 0.001$).

The ROC analysis specifically performed on HF showed that HF < 30 could divide MNV eyes into 2 clinically different subgroups, with 0.667 sensitivity and 0.534 specificity, turning out to be less sensitive overall than MNV VT in separating a different functional outcome in MNV subgroups.

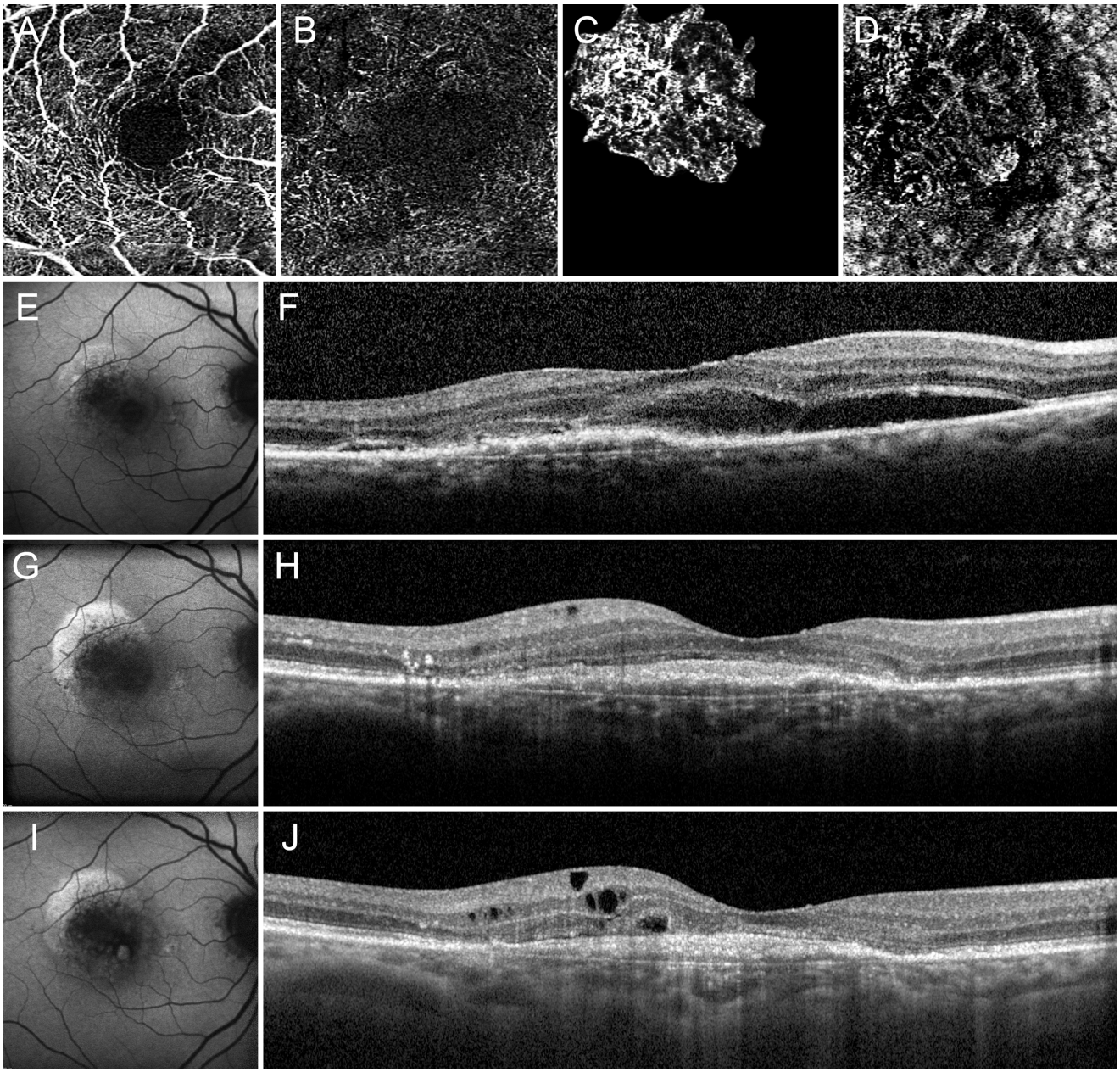

Figure 6. Type 1 MNV case classified as group 2 (VT > 8.40). OCTA clearly reconstructs SCP (**A**), DCP (**B**), MNV (**C**), and CC (**D**). Baseline features are shown in (**E**) and (**F**). Exudation was found to have diminished markedly following anti-VEGF treatment. However, the onset and progression of outer retinal atrophy are clearly visible, together with the development of intraretinal cysts associated with progressively deteriorating conditions at both the 1-year (**G, H**) and 2-year (**I, J**) follow-ups.

All the measures performed showed high reproducibility and repeatability, as reported in Table 3.

Discussion

Type 1 MNV is a common manifestation of advanced AMD and leads to visual acuity loss. The possibility of multimodal imaging to predict the final visual outcome of patients treated with intravitreal anti-VEGF is still some way off; there do exist a number of biomarkers,[4–6] although, as yet, there are no specific correlations with MNV activity.

In our study, quantitative OCTA assessment enabled two clinically different subgroups of patients affected by type 1 MNV to be identified: a low VT and a high VT subgroup, the former with better clinical

Table 2. Sub-Group Analysis of Type 1 MNV (VT Cutoff = 8.40)

Sub-Group Analysis of Type 1 MNV (VT Cutoff = 8.40)					
	Group 1 (45 Eyes) (VT < 8.40)		Group 2 (46 Eyes) (VT > 8.40)		
	Mean	STD	Mean	STD	*P* Value
Age	76.70	8.17	78.83	5.91	>0.05
Sex (M/F)	24/21		25/21		>0.05
BCVA logMAR baseline	0.47	0.47	0.47	0.47	>0.05
BCVA logMAR 2 y	0.22	0.21	0.41	0.30	<0.01*
No. of intravitreal injections 2 y	12.11	2.22	11.66	1.98	>0.05
CMT baseline	394.42	85.07	353.55	82.06	<0.05*
CMT 2 y	363.99	86.20	330.29	81.71	>0.05
VD SCP baseline	0.38	0.03	0.38	0.02	>0.05
VD DCP baseline	0.37	0.03	0.36	0,03	>0.05
VD CC baseline	0.45	0.05	0.46	0.03	>0.05
VT MNV baseline	7.58	0.42	9.59	1.30	<0.01*
VDisp MNV baseline	23.35	9.02	22.30	6.89	>0.05
Blooding at baseline	3.7%		8.19%		
Pigment epithelium detachment at baseline	34.75%		40.87%		
Subretinal fluid at baseline	43.95%		41.90%		
Photoreceptors stretch at baseline	36.81%		25.55%		
Subretinal fibrosis at 2 y follow-up	6.13%		15.32%		
Outer retinal atrophy at 2 y follow-up	8.18%		23.51%		

Table 3. Reproducibility and Repeatability of OCTA Quantitative Parameters

Reproducibility and Repeatability of OCTA Quantitative Parameters		
Parameter	Reproducibility	Repeatability
VD SCP	0.96	0.95
VD DCP	0.91	0.90
VD CC	0.98	0.98
VT MNV	0.95	0.93
VDisp MNV	0.92	0.91

features than the latter. These groups differed significantly in terms of visual outcome after 2 years of treatment, as well as with regard to the development of degenerative retinal features, including subretinal fibrosis and outer retinal atrophy. Specifically, the low VT subgroup displayed better final visual outcomes along with less severe signs of degenerative outer retinal alterations. Interestingly, the low VT subgroup showed worse baseline BCVA than the high VT subgroup, although this difference was not statistically significant. This finding might be explained by the greater incidence of photoreceptor elongation found in the low VT subgroup, possibly due to photoreceptor distress, together with the better anatomic as well as functional recovery after treatment. Our ROC analysis exhibited the same MNV VT cutoff already found in our previous investigation.[7] It is worth noting that both subgroups required a similar number of intravitreal injections. MNV showing higher VT may therefore be characterized by a more florid and more alarming neovascular network. Indeed, as previously reported, VT may be considered a measure of the amount of perfusion involving the retinal vascular network.[16] In addition, the higher VT might be predictive of a more likely development of subretinal fibrosis and outer retinal atrophy – conditions leading to a worse visual outcome after 2 years of follow-up. It is also noteworthy that the two subgroups did not differ at baseline in terms of retinal/subretinal hemorrhages, pigment epithelium detachment, and subretinal fluid, suggesting that these biomarkers are less strictly related to

anatomic and functional outcomes than VT. Intraretinal HF represents a valid biomarker of the MNV's response to treatment, HF reduction after treatment being related to better functional and anatomic outcomes. However, ROC analyses revealed that HF proved less reliable than MNV VT in differentiating clinically relevant MNV subgroups.

We are aware that our study has several limitations and should be viewed as merely a preliminary study outlining a possible approach that may be taken up by larger surveys with longer-term follow-ups. Moreover, quantitative OCTA analyses depend on high-quality images and can be affected by artifacts, as well as being more difficult in the presence of retinal angiomatous proliferation, polypoidal choroidal vasculopathy, or high PED.[18–20] Mindful of this, all precautions were taken to minimize potential pitfalls. We further acknowledge that pathogenetic mechanisms hypothesized on the basis of our imaging-based findings would need histopathological validation. Our study cannot claim to have reached any definitive conclusions as it did not analyze enough cases and its follow-up was too short. Another weakness is the simple binary classification of clinical data (atrophy, fibrosis, and hemorrhage) that was adopted in preference to a precise quantification.

Last, it is our intention to complete our analyses by including the OCTA parameters during the follow-up and at the end of the follow-up. We have been following the patients in order to obtain these data, but they are very difficult to interpret owing to the various changes that occur with the passage of time. As a result, we believe that although baseline MNV analyses using quantitative OCTA parameters can yield some useful prognostic pointers, follow-up research may need more advanced technological tools.

In essence, the present study showed that a quantitative OCTA categorization of type 1 MNV secondary to AMD can provide useful information in terms of clinical and functional outcomes after anti-VEGF treatment. In anticipation of future artificial intelligence-based assessments, the adoption of a quantitative-based MNV subclassification might help improve patient categorization, reducing the inherent shortcomings of subjective evaluation. Further studies are warranted to confirm our findings.

Acknowledgments

Disclosure: **A. Arrigo,** None; **E. Aragona,** None; **C. Di Nunzio,** None; **F. Bandello,** Alcon (C), Alimera Sciences (C), Allergan Inc. (C), Farmila-Thea (C), Bayer Shering-Pharma (C), Bausch and Lomb (C), Genentech (C), Hoffmann-La Roche (C), NovagaliPharma (C), Novartis (C), Sanofi-Aventis (C), Thrombogenics (C), Zeiss (C); **M. B. Parodi,** None

References

1. Jung JJ, Chen CY, Mrejen S, et al. The incidence of neovascular subtypes in newly diagnosed neovascular age-related macular degeneration. *Am J Ophthalmol*. 2014;158:769–779.e2.
2. Schmidt-Erfurth U, Chong V, Loewenstein A, et al. Guidelines for the management of neovascular age-related macular degeneration by the European Society of Retina Specialists (EURETINA). *Br J Ophthalmol*. 2014;98:1144–1167.
3. Farecki ML, Gutfleisch M, Faatz H, et al. Characteristics of type 1 and 2 MNV in exudative AMD in OCT-Angiography. *Graefes Arch Clin Exp Ophthalmol*. 2017;255:913–921.
4. Al-Sheikh M, Iafe NA, Phasukkijwatana N, Sadda SR, Sarraf D. Biomarkers of neovascular activity in age-related macular degeneration using optical coherence tomography angiography. *Retina*. 2018;38:220–230.
5. Coscas F, Cabral D, Pereira T, et al. Quantitative optical coherence tomography angiography biomarkers for neovascular age-related macular degeneration in remission. *PLoS One*. 2018;13:e0205513.
6. Xu D, Dávila JP, Rahimi M, et al. Long-term progression of type 1 neovascularization in age-related macular degeneration using optical coherence tomography angiography. *Am J Ophthalmol*. 2018;187:10–20.
7. Arrigo A, Romano F, Aragona E, et al. Optical coherence tomography angiography can categorize different subgroups of choroidal neovascularization secondary to age-related macular degeneration. *Retina*, https://doi.org/10.1097/IAE.0000000000002775.
8. Mrejen S, Giocanti-Auregan A, Tabary S, Cohen SY. Sensitivity of 840-nm spectral domain optical coherence tomography angiography in detecting type 1 neovascularization according to the height of the associated pigment epithelial detachment. *Retina*. 2019;39:1973–1984.
9. Tomita Y, Kubis N, Calando Y. Long-term in vivo investigation of mouse cerebral microcirculation by fluorescence confocal microscopy in the area of focal ischemia. *J Cereb Blood Flow Metab*. 2005;25:858–967.

10. Goldman D, Popel AS. A computational study of the effect of capillary network anastomosis and tortuosity on oxygen transport. *J Theor Biol*. 2000;206:181–194.
11. Arganda-Carreras I, Fernández-González R, Muñoz-Barrutia A, Ortiz-De-Solorzano C. 3D reconstruction of histological sections: application to mammary gland tissue. *Microsc Res Tech*. 2010;73:1019–1029.
12. Grisan E, Foracchia M, Ruggeri A. A novel method for the automatic grading of retinal vessel tortuosity. *IEEE Trans Med Imaging*. 2008;27:310–319.
13. Righi M, Locatelli SM, Carlo-Stella C, et al. Vascular amounts and dispersion of caliber-classified vessels as key parameters to quantitate 3D microangioarchitectures in multiple myeloma experimental tumors. *Sci Rep*. 2018;8:17520.
14. Konerding MA, Malkusch W, Klapthor B, et al. Evidence for characteristic vascular patterns in solid tumours: quantitative studies using corrosion casts. *Br J Cancer*. 1999;80:724–732.
15. Manikandan S. Measures of dispersion. *J Pharmacol Pharmacother*. 2011;2:315–316.
16. Liu ZQ. Scale space approach to directional analysis of images. *Appl Opt*. 1991;30:1369–1373.
17. British Standards Institution. *Precision of Test Methods I: Guide for the Determination and Reproducibility for a Standard Test Method (BS 5497, Part I)*. London: BSI; 1979.
18. Arrigo A, Aragona E, Capone L, et al. Advanced optical coherence tomography angiography analysis of age-related macular degeneration complicated by onset of unilateral choroidal neovascularization. *Am J Ophthalmol*. 2018;195:233–242.
19. Spaide RF, Fujimoto JG, Waheed NK. Image artifacts in optical coherence tomography angiography. *Retina*. 2015;35:2163–2180.
20. Spaide RF, Fujimoto JG, Waheed NK, Sadda SR, Staurenghi G. Optical coherence tomography angiography. *Prog Retin Eye Res*. 2018;64:1–55.